- According to (17.104), the enhancement of the density of states at the Fermi energy is

$$\begin{aligned}\rho^*(0) &= \rho + \frac{\Delta}{\pi(\Delta^2+\lambda^2)} \\ &= \rho + \frac{\sin^2(\pi q)}{\pi T_K}\end{aligned} \tag{17.112}$$

per spin channel. When the temperature is changed or a magnetic field is introduced, one can neglect changes in Δ and λ, since the free energy is stationary. This implies that, in the large-N limit, the susceptibility and linear specific heat are those of a non-interacting resonance of width Δ. The change in linear specific heat $\Delta C_V = \Delta\gamma T$ and the change in the paramagnetic susceptibility $\Delta\chi$ are given by

$$\begin{aligned}\Delta\gamma &= \left[\frac{N\pi^2 k_B^2}{3}\right]\rho_i(0) = \left[\frac{N\pi^2 k_B^2}{3}\right]\frac{\sin^2(\pi q)}{\pi T_K} \\ \Delta\chi &= \left[N\frac{j(j+1)(g\mu_B)^2}{3}\right]\rho_i(0) = \left[N\frac{j(j+1)(g\mu_B)^2}{3}\right]\frac{\sin^2(\pi q)}{\pi T_K}.\end{aligned} \tag{17.113}$$

Notice how it is the Kondo temperature that determines the size of these two quantities. The dimensionless Wilson ratio of these two quantities is

$$W = \left[\frac{(\pi k_B)^2}{(g\mu_B)^2 j(j+1)}\right]\frac{\Delta\chi}{\Delta\gamma} = 1.$$

At finite N, fluctuations in the mean-field theory can no longer be ignored. These fluctuations induce *interactions* among the quasiparticles, and the Wilson ratio becomes

$$W = \frac{1}{1-\frac{1}{N}}.$$

The dimensionless Wilson ratios of a large variety of heavy-electron materials lie remarkably close to this value.

17.6 Mean-field theory of the Kondo lattice

17.6.1 Diagonalization of the Hamiltonian

We can now make the jump from the single-impurity problem to the lattice. The virtue of the large-N method is that, while approximate, it can be readily scaled up to the lattice. We'll now recompute the effective action for the lattice, using equation (17.70). Let us assume that the hybridization and constraint fields at the saddle point are uniform, with $V_j = V$ and $\lambda_j = \lambda$ at every site. In fact, even if we start with a $V_j = Ve^{-i\phi j}$ with a different phase at each site, we can always absorb the phase ϕ_j using the Read–Newns gauge transformation (17.57) to absorb the additional phase onto the f-electron field. We

then have a translationally invariant mean-field Hamiltonian. We begin by rewriting the mean-field Hamiltonian in momentum space as follows:

$$H_{MFT} = \sum_{\mathbf{k}\sigma} \left(c^\dagger_{\mathbf{k}\sigma}, f^\dagger_{\mathbf{k}\sigma}\right) \overbrace{\begin{pmatrix} \epsilon_{\mathbf{k}} & V \\ \bar{V} & \lambda \end{pmatrix}}^{\underline{h}(\mathbf{k})} \begin{pmatrix} c_{\mathbf{k}\sigma} \\ f_{\mathbf{k}\sigma} \end{pmatrix} + N\mathcal{N}_s \left(\frac{|V|^2}{J} - \lambda q\right) \tag{17.114}$$

$$= \sum_{\mathbf{k}\sigma} \psi^\dagger_{\mathbf{k}\sigma}\, \underline{h}(\mathbf{k})\, \psi_{\mathbf{k}\sigma} + N\mathcal{N}_s \left(\frac{|V|^2}{J} - \lambda q\right).$$

Here, $f^\dagger_{\mathbf{k}\sigma} = \frac{1}{\sqrt{\mathcal{N}_s}} \sum_j f^\dagger_{j\sigma} e^{i\mathbf{k}\cdot\mathbf{R}_j}$ is the Fourier transform of the f-electron field and we have introduced the two-component notation

$$\psi_{\mathbf{k}\sigma} = \begin{pmatrix} c_{\mathbf{k}\sigma} \\ f_{\mathbf{k}\sigma} \end{pmatrix}, \qquad \psi^\dagger_{\mathbf{k}\sigma} = \left(c^\dagger_{\mathbf{k}\sigma}, f^\dagger_{,\mathbf{k}\sigma}\right), \qquad \underline{h}(\mathbf{k}) = \begin{pmatrix} \epsilon_{\mathbf{k}} & V \\ \bar{V} & \lambda \end{pmatrix}. \tag{17.115}$$

We should think of H_{MFT} as a renormalized Hamiltonian, describing the low-energy quasiparticles moving through a self-consistently determined array of resonant scattering centers. Later, we will see that the f-electron operators are composite objects, formed as bound states between spins and conduction electrons.

The mean-field Hamiltonian can be diagonalized in the form

$$H_{MFT} = \sum_{\mathbf{k}\sigma} \left(a^\dagger_{\mathbf{k}\sigma}, b^\dagger_{\mathbf{k}\sigma}\right) \begin{pmatrix} E_{\mathbf{k}^+} & 0 \\ 0 & E_{\mathbf{k}^-} \end{pmatrix} \begin{pmatrix} a_{\mathbf{k}\sigma} \\ b_{\mathbf{k}\sigma} \end{pmatrix} + Nn \left(\frac{\bar{V}V}{J} - \lambda q\right). \tag{17.116}$$

Here $a^\dagger_{\mathbf{k}\sigma} = u_{\mathbf{k}} c^\dagger_{\mathbf{k}\sigma} + v_{\mathbf{k}} f^\dagger_{\mathbf{k}\sigma}$ and $b^\dagger_{\mathbf{k}\sigma} = -v_{\mathbf{k}} c^\dagger_{\mathbf{k}\sigma} + u_{\mathbf{k}} f^\dagger_{\mathbf{k}\sigma}$ are linear combinations of $c^\dagger_{\mathbf{k}\sigma}$ and $f^\dagger_{\mathbf{k}\sigma}$, playing the role of quasiparticle operators with corresponding energy eigenvalues

$$\det\left[E^{\pm}_{\mathbf{k}} \underline{1} - \begin{pmatrix} \epsilon_{\mathbf{k}} & V \\ \bar{V} & \lambda \end{pmatrix}\right] = (E_{\mathbf{k}\pm} - \epsilon_{\mathbf{k}})(E_{\mathbf{k}\pm} - \lambda) - |V|^2 = 0 \tag{17.117}$$

or

$$E_{\mathbf{k}\pm} = \frac{\epsilon_{\mathbf{k}} + \lambda}{2} \pm \left[\left(\frac{\epsilon_{\mathbf{k}} - \lambda}{2}\right)^2 + |V|^2\right]^{\frac{1}{2}}, \tag{17.118}$$

and eigenvectors taking the BCS form

$$\left\{ \begin{array}{c} u_{\mathbf{k}} \\ v_{\mathbf{k}} \end{array} \right\} = \left[\frac{1}{2} \pm \frac{(\epsilon_{\mathbf{k}} - \lambda)/2}{2\sqrt{\left(\frac{\epsilon_{\mathbf{k}} - \lambda}{2}\right)^2 + |V|^2}}\right]^{\frac{1}{2}}. \tag{17.119}$$

The hybridized dispersion described by these energies is shown in Figure 17.10.

Note the following:

- Hybridization builds an upper and a lower band, separated by a *direct* hybridization gap of size $2V$ and a much smaller *indirect* gap. If we put $\epsilon_{\mathbf{k}} = \pm D$, we see that the upper and lower edges of the gap are given by

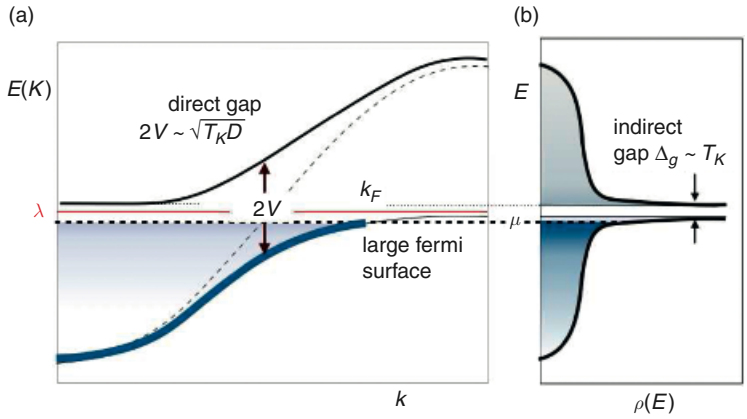

(a) Dispersion for the Kondo lattice mean-field theory. (b) Renormalized density of states, showing hybridization gap Δ_g. **Fig. 17.10**

$$E^{\pm} = \frac{\mp D + \lambda}{2} \pm \sqrt{\left(\frac{\mp D - \lambda}{2}\right)^2 + V^2} \approx \lambda \pm \frac{V^2}{D} \qquad (D >> \lambda), \tag{17.120}$$

so the indirect gap has a size $\Delta_g \sim 2V^2/D$, where D is the half-bandwidth. From our mean-field solution to the Kondo impurity problem, we can anticipate $V^2/D \sim V^2\rho \sim T_K$, so that $\Delta_g \sim T_K$, the single-ion Kondo temperature, which implies that $V \sim \sqrt{T_K D}$.

- In the special case when the chemical potential lies in the gap, a *Kondo* insulator is formed.
- The effective mass of the Fermi surface is *opposite* to the conduction sea, so a conduction sea of electrons is transformed into a heavy-fermion sea of holes.
- The Fermi surface volume *expands* in response to the formation of heavy electrons (see Figure 17.11). The enlarged Fermi surface volume now counts the total number of occupied quasiparticle states,

$$N_{tot} = \langle \sum_{k\lambda\sigma} n_{k\lambda\sigma} \rangle = \langle \hat{n}_f + \hat{n}_c \rangle, \tag{17.121}$$

where $n_{k\lambda\sigma} = a^{\dagger}_{k\lambda\sigma} a_{k\lambda\sigma}$ is the number operator for the quasiparticles and n_c is the total number of conduction electrons. This means

$$N_{tot} = N \frac{V_{FS} a^3}{(2\pi)^3} = Q + n_c, \tag{17.122}$$

where a^3 is the volume of the unit cell. This is rather remarkable, for the expansion of the Fermi surface implies an increased charge density in the Fermi sea. Since charge is conserved, we are forced to conclude that there is a compensating $+Q|e|$ charge density per unit cell provided by the Kondo singlets formed at each site, as illustrated in Figure 17.11.

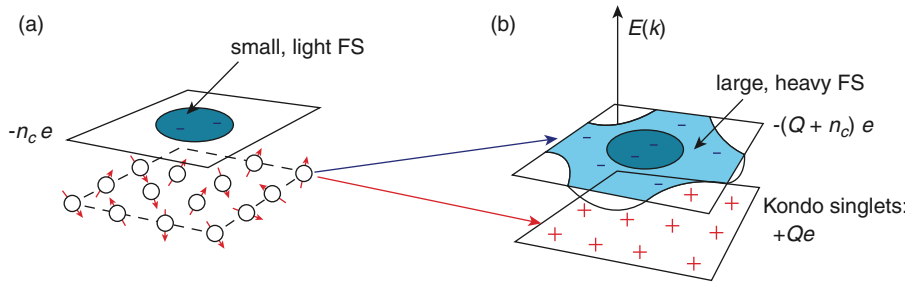

Fig. 17.11 Spin quenching in the Kondo lattice: (a) high-temperature state: small Fermi surface (FS) with a background of spins; (b) low-temperature state where a large Fermi surface develops against a background of positive charge. Each spin "ionizes" into Q heavy electrons, leaving behind a background of Kondo singlets, each with charge $+Qe$.

- We can construct the mean-field ground state from the quasiparticle operators, as follows:

$$|MF\rangle = \prod_{|\mathbf{k}|<k_F\sigma} b^\dagger_{\mathbf{k}\sigma}|0\rangle = \prod_{|\mathbf{k}|<k_F\sigma} (-v_{\mathbf{k}} c^\dagger_{\mathbf{k}\sigma} + u_{\mathbf{k}} f^\dagger_{\mathbf{k}\sigma})|0\rangle. \tag{17.123}$$

However, this state only satisfies the constraint on the average. We can improve it by imposing the constraint, forming a *Gutzwiller wavefunction* [36–38],

$$|GW\rangle = P_Q \prod_{|\mathbf{k}|<k_F\sigma} (-v_{\mathbf{k}} c^\dagger_{\mathbf{k}\sigma} + u_{\mathbf{k}} f^\dagger_{\mathbf{k}\sigma})|0\rangle, \tag{17.124}$$

where, using (17.48),

$$P_Q = \prod_j P_Q(j) = \int_0^{2\pi} \prod_j \frac{d\alpha_j}{2\pi} e^{i\sum_j \alpha_j(\hat{n}_f(j)-Q)}. \tag{17.125}$$

The action of the constraint gives rise to a highly incompressible Fermi liquid, in which the compressibility is far smaller than the density of states.

17.6.2 Mean-field free energy and saddle point

Let us now use the results of the previous section to calculate the mean-field free energy F_{MFT} and determine self-consistently the parameters λ and V which set the scales of the Kondo lattice. Using (17.70) we obtain

$$F_{MF} = -NT \sum_{\mathbf{k}, i\omega_r} \mathrm{Tr} \ln \overbrace{\left[-i\omega_r + \begin{pmatrix} \epsilon_{\mathbf{k}} & V \\ V & \lambda \end{pmatrix}\right]}^{-\mathcal{G}^{-1}_{\mathbf{k}}(i\omega_r)} + \mathcal{N}_s \left(\frac{N|V|^2}{J} - \lambda Q\right), \tag{17.126}$$

where $\mathcal{N}_s$ is the number of sites in the lattice. Note that translational invariance means that momentum is conserved and the Green's function is diagonal in momentum, so we can rewrite the trace over the momentum as a sum over $\mathbf{k}$. Let us remind ourselves of the steps

taken between (17.70) and (17.71). We begin by re-writing the trace of the logarithm as a determinant, which we then factorize in terms of the energy eigenvalues:

$$\mathrm{Tr}\ln\left[-i\omega_r\underline{1}+\begin{pmatrix}\epsilon_{\mathbf{k}} & V\\ V & \lambda\end{pmatrix}\right]=\ln\det\left[-z\underline{1}+\begin{pmatrix}\epsilon_{\mathbf{k}} & V\\ V & \lambda\end{pmatrix}\right]=\ln\left[\overbrace{(\epsilon_{\mathbf{k}}-i\omega_r)(\lambda-i\omega_r)-V^2}^{(E_{\mathbf{k}+}-i\omega_r)(E_{\mathbf{k}-}-i\omega_r)}\right]$$
$$=\sum_{n=\pm}\ln(E_{\mathbf{k}n}-i\omega_r). \tag{17.127}$$

Next, by carrying out the summation over Matsubara frequencies, using the result $-T\sum_{i\omega_r}\ln(E_{\mathbf{k}n}-i\omega_r)=-T\ln(1+e^{-\beta E_{\mathbf{k}n}})$, we obtain

$$\frac{F}{N}=-T\sum_{\mathbf{k},\pm}\ln\left[1+e^{-\beta E_{\mathbf{k}\pm}}\right]+\mathcal{N}_s\left(\frac{V^2}{J}-\lambda q\right). \tag{17.128}$$

Let us discuss the ground state, in which only the lower band contributes to the free energy. As $T\to 0$, we can replace $-T\ln(1+e^{-\beta E_{\mathbf{k}}})\to\theta(-E_{\mathbf{k}})E_{\mathbf{k}}$, so the ground-state energy $E_0=F(T=0)$ involves an integral over the occupied states of the lower band:

$$\frac{E_0}{N\mathcal{N}_s}=\int_{-\infty}^{0}dE\rho^*(E)E+\left(\frac{V^2}{J}-\lambda q\right), \tag{17.129}$$

where we have introduced the density of heavy-electron states $\rho^*(E)=\sum_{\mathbf{k},\pm}\delta(E-E_{\mathbf{k}}^{(\pm)})$. Now by (17.117) the relationship between the energy E of the heavy electrons and the energy ϵ of the conduction electrons is

$$E=\epsilon+\frac{V^2}{E-\lambda}.$$

As we sum over momenta $\mathbf{k}$ within a given energy shell, there is a one-to-one correspondence between each conduction electron state and each quasiparticle state, so we can write $\rho^*(E)dE=\rho(\epsilon)d\epsilon$, where the density of heavy-electron states is

$$\rho^*(E)=\rho\frac{d\epsilon}{dE}=\rho\left(1+\frac{V^2}{(E-\lambda)^2}\right). \tag{17.130}$$

Here we have approximated the underlying conduction electron density of states by a constant $\rho=1/(2D)$. The originally flat conduction electron density of states is now replaced by a hybridization gap, flanked by two sharp peaks of approximate width $\pi\rho V^2\sim T_K$ (Figure 17.10). Note that the lower bandwidth is lowered by an amount $-V^2/D$. With this information, we can carry out the integral over the energies, to obtain

$$\frac{E_0}{N\mathcal{N}_s}=\rho\int_{-D-V^2/D}^{0}dEE\left(1+\frac{V^2}{(E-\lambda)^2}\right)+\left(\frac{V^2}{J}-\lambda q\right), \tag{17.131}$$

where we have assumed that the upper band is empty and the lower band is partially filled. Carrying out the integral, we obtain

$$\frac{E_0}{N\mathcal{N}_s} = -\frac{\rho}{2}\left(D + \frac{V^2}{D}\right)^2 + \frac{\Delta}{\pi}\int_{-D}^{0} dE\left(\frac{1}{E-\lambda} + \frac{\lambda}{(E-\lambda)^2}\right) + \left(\frac{V^2}{J} - \lambda q\right)$$
$$= -\frac{D^2\rho}{2} + \frac{\Delta}{\pi}\ln\left(\frac{\lambda}{D}\right) + \left(\frac{V^2}{J} - \lambda q\right), \tag{17.132}$$

where we have replaced $\Delta = \pi\rho V^2$ and have dropped terms of order $O(\Delta^2/D)$. We can rearrange this expression, absorbing the bandwidth D and Kondo coupling constant into a single Kondo temperature $T_K = De^{-\frac{1}{J\rho}}$, as follows:

$$\begin{aligned}\frac{E_0}{N\mathcal{N}_s} &= -\frac{D^2\rho}{2} + \frac{\Delta}{\pi}\ln\left(\frac{\lambda}{D}\right) + \left(\frac{\pi\rho V^2}{\pi\rho J} - \lambda q\right)\\ &= -\frac{D^2\rho}{2} + \frac{\Delta}{\pi}\ln\left(\frac{\lambda}{D}\right) + \left(\frac{\Delta}{\pi\rho J} - \lambda q\right)\\ &= -\frac{D^2\rho}{2} + \frac{\Delta}{\pi}\ln\left(\frac{\lambda}{De^{-\frac{1}{J\rho}}}\right) - \lambda q\\ &= -\frac{D^2\rho}{2} + \frac{\Delta}{\pi}\ln\left(\frac{\lambda}{T_K}\right) - \lambda q.\end{aligned} \tag{17.133}$$

This describes the energy of a family of Kondo lattice models with different $J(D)$ and cutt-off D, but fixed Kondo temperature. If we impose the constraint $\frac{\partial E_0}{\partial \lambda} = \langle n_f\rangle - Q = 0$, we obtain $\frac{\Delta}{\pi\lambda} - q = 0$, so

$$\frac{E_0(V)}{N\mathcal{N}_s} = \frac{\Delta}{\pi}\ln\left(\frac{\Delta}{\pi q e T_K}\right) - \frac{D^2\rho}{2} \qquad (\Delta = \pi\rho|V|^2). \tag{17.134}$$

Let us pause for a moment to consider this energy functional qualitatively. There are two points to be made:

- The energy surface $E_0(V)$ is actually independent of the phase of $V = |V|e^{i\phi}$(see Figure 17.12), and has the form of a "Mexican hat" (Figure 17.12) at low temperatures. The minimum of this functional will then determine a familiy of saddle-point values $V = |V_0|e^{i\phi}$, where ϕ can have any value. If we differentiate the ground-state energy with respect to Δ, we obtain

  $$0 = \frac{1}{\pi}\ln\left(\frac{\Delta}{\pi q T_K}\right)$$

  or

  $$\Delta = \pi q T_K,$$

  confirming that $\Delta \sim T_K$.
- The mean-field value of the constraint field λ is determined relative to the Fermi energy μ. Were we to introduce a slowly varying external potential field to the conduction electron sea, then the chemical potential would be locally shifted so that $\mu \to \mu + e\phi(t)$. So long as the field $\phi(t)$ is varied at a rate that is slow compared with the Kondo temperature, the constraint field will always track with the chemical potential, and, since the constraint field is pinned to the chemical potential, $\lambda \to \lambda + e\phi(t)$. In the process, the constraint term will become

  $$\lambda(\hat{n}_f(j) - Q) \to \lambda(\hat{n}_f(j) - Q) + e\phi(t)(\hat{n}_f(j) - Q). \tag{17.135}$$

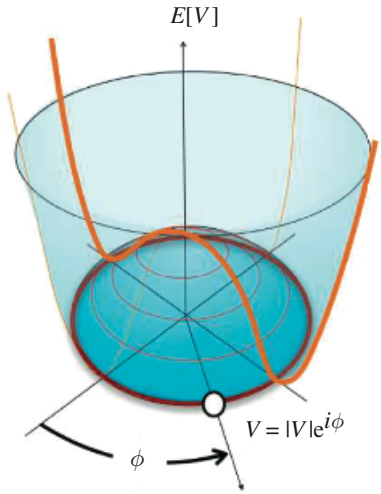

"Mexican hat" potential for the Kondo Lattice, evaluated at constant $\langle n_f \rangle = Q$ as a function of a complex hybridization $V = |V|e^{i\phi}$. Fig. 17.12

Since the f-electrons now couple to the external potential $e\phi$ we have to ascribe a physical charge $e = -|e|$ to them. By contrast, the $-Q$ term in the constraint must be interpreted as a *background positive charge* $|e|Q \equiv |e|$ per site. These lines of reasoning indicate that we should think of the Kondo effect as a *many-body ionization phenomenon*, in which the neutral local moment splits up into a negatively charged heavy electron and a stationary positive background charge that we can associate with the formation of a Kondo singlet.

17.6.3 Kondo lattice Green's function

Let's now take a look at the matrix Green's function, given by

$$\mathcal{G}_{\mathbf{k}}(\tau) = -\langle \psi_{\mathbf{k}\sigma}(\tau)\psi^{\dagger}_{\mathbf{k}\sigma}(0)\rangle \equiv \begin{bmatrix} G_c(\mathbf{k},\tau) & G_{cf}(\mathbf{k},\tau) \\ G_{fc}(\mathbf{k},\tau) & G_f(\mathbf{k},\tau) \end{bmatrix}, \tag{17.136}$$

where $G_c(\mathbf{k},\tau) = -\langle c_{\mathbf{k}}(\tau)c^{\dagger}_{\mathbf{k}\sigma}(0)\rangle$, $G_{cf}(\mathbf{k},\tau) = -\langle c_{\mathbf{k}}(\tau)f^{\dagger}_{\mathbf{k}\sigma}(\tau)\rangle$, and so on. The anomalous off-diagonal members of this Green's function remind us of the Gor'kov functions in BCS theory, and develop with the coherent hybridization. Using the two-component notation (17.115), and the results of Section 12.4.3, this Green's function can be written

$$\mathcal{G}_{\mathbf{k}}(\tau) = -(\partial_\tau + \underline{h}_{\mathbf{k}})^{-1} \xrightarrow{\text{F.T.}} \mathcal{G}_{\mathbf{k}}(z) = (z - \underline{h}_{\mathbf{k}})^{-1} \tag{17.137}$$

or, more explicitly,

$$\begin{aligned} \mathcal{G}_{\mathbf{k}}(z) = (z - \underline{h}_{\mathbf{k}})^{-1} &= \begin{pmatrix} z-\epsilon_{\mathbf{k}} & -V \\ -V & z-\lambda \end{pmatrix}^{-1} = \begin{pmatrix} G_c(\mathbf{k},z) & G_{cf}(\mathbf{k},z) \\ G_{fc}(\mathbf{k},z) & G_f(\mathbf{k},z) \end{pmatrix} \\ &= \frac{1}{(z-\epsilon_{\mathbf{k}})(z-\lambda) - V^2} \begin{pmatrix} z-\lambda & V \\ V & z-\epsilon_{\mathbf{k}} \end{pmatrix}, \end{aligned} \tag{17.138}$$

where we have taken the liberty of analytically extending $i\omega_r \to z$ into the complex plane. Now we can read off the Green's functions. In particular, the hybridized conduction electron Green's function is

$$G_c(\mathbf{k}, z) = \quad = \frac{z-\lambda}{(z-\epsilon_{\mathbf{k}})(z-\lambda)-V^2}$$
$$= \frac{1}{z-\epsilon_{\mathbf{k}}-\frac{V^2}{z-\lambda}} \equiv \frac{1}{z-\epsilon_{\mathbf{k}}-\Sigma_c(z)}, \tag{17.139}$$

which we can interpret physically as conduction electrons scattering off resonant f-states at each site, giving rise to a momentum-conserving self-energy:

$$\Sigma_c(z) = \quad = \frac{V^2}{z-\lambda}. \tag{17.140}$$

$O(1)$

We can treat this process as a pole at energy $z = \lambda$ in the condution t-matrix. We shall argue later that this pole represents the formation of a composite fermion. A similar process occurs in the impurity Kondo model, but in that case the scattering is local, and connects all wavevectors, whereas in the lattice, coherence implies momentum is conserved. Notice that the denominator in each of the Green's functions involves the same quasiparticle poles, since $(z-\epsilon_{\mathbf{k}})(z-\lambda)-V^2 = (z-E^+_{\mathbf{k}})(z-E^-_{\mathbf{k}})$, and hence near the Fermi surface at $E_{\mathbf{k}_F} = 0$ the conduction Green's function can be written

$$G_c(z \sim E_{\mathbf{k}}) = \frac{Z_{\mathbf{k}}}{z-E^-_{\mathbf{k}}}, \tag{17.141}$$

where

$$Z_{\mathbf{k}} = (1-\partial_z\Sigma_c(z))^{-1}\,|_{z=0} = \frac{1}{1+\frac{V^2}{\lambda^2}} \sim \frac{T_K}{D} \sim \frac{m}{m^*} << 1, \tag{17.142}$$

where we have identified the scales $V^2/D \sim T_K$ (hence $V^2 \sim DT_K$) and $\lambda \sim T_K$ with the single-ion Kondo temperature. We see that the strength of the quasiparticle pole in the conduction electrons, related to the mass renormalization, is very small.

Similarly, the f-Green's function is

$$G_f(\mathbf{k}, z) = \quad = \frac{z-\epsilon_{\mathbf{k}}}{(z-\epsilon_{\mathbf{k}})(z-\lambda)-V^2} = \frac{1}{i\omega_r-\lambda-\frac{V^2}{z-\epsilon_{\mathbf{k}}}}. \tag{17.143}$$

Finally, the *anomalous* Green's functions are given by

$$G_{cf}(\mathbf{k}, z) = \quad = \frac{1}{z-\epsilon_{\mathbf{k}}} V G_f(\mathbf{k}, i\omega_n) = \frac{V}{(z-\epsilon_{\mathbf{k}})(z-\lambda)-V^2}, \tag{17.144}$$

which we can interpret as the result of hybridization. We will return to use these expressions to calculate the low-energy part of the tunneling spectrum.

17.7 Kondo insulators

The Kondo insulator is the simplest version of the Kondo lattice, in which the formation of Kondo singlets leads to a fully gapped, insulating state. While the term "Kondo insulator" dates back to the early 1990s [5], these are the oldest heavy-fermion materials. The first heavy-fermion or Kondo insulator, SmB_6, was discovered in 1969 by Menth, Buehler, and Geballe at AT&T Bell Laboratories [6], followed closely by SmS under pressure [7]. It was these materials that inspired Neville Mott to propose that Kondo insulators involve a kind of excitonic ordering between localized f-electrons and conduction electrons [8], driving the emergent hybridization that we have been discussing. A predecessor of the large-N path integral approach to Kondo insulators was proposed in 1979 by Claudine Lacroix and Michel Cyrot at the Laboratoire Louis Néel in Grenoble [28]. At the time of writing this book, SmB_6 has once again been thrust into the main-stream of research, with the proposal [39] that this is an example of a topological insulator – a *topological Kondo insulator* with robust conducting surfaces [40, 41]. This is a topic we will return to in Chapter 18 when we consider mixed valence.

17.7.1 Strong-coupling expansion

In many ways, the Kondo insulator is the simplest ground state of the Kondo lattice. Let us begin by returning to the $SU(2)$ Kondo lattice model:

$$H = -t\sum_{(i,j)\sigma}(c^\dagger_{i\sigma}c_{j\sigma} + \text{H.c.}) + J\sum_{j,\alpha\beta}\vec{\sigma}_j\cdot\vec{S}_j \qquad (\vec{\sigma}_j \equiv (c^\dagger_{j\beta}\vec{\sigma}_{\beta\alpha}c_{j\alpha})), \tag{17.145}$$

corresponding to a tight-binding Kondo lattice where the electrons at each site are coupled antiferromagnetically to a local moment. We can gain a lot of insight by examining the strong-coupling limit, in which the dispersion of the conduction sea is much smaller than J, so that $t/J << 1$ is a small parameter. In this limit, the intersite hopping is a perturbation to the onsite Kondo insteraction:

$$H \overset{t/J\to 0}{\longrightarrow} J\sum_{j,\alpha\beta}\vec{\sigma}_j\cdot\vec{S}_j + O(t), \tag{17.146}$$

and the ground state corresponds to the formation of a spin singlet at each site, denoted by the wavefunction

$$|KI\rangle = \prod_j \frac{1}{\sqrt{2}}\Big(\Uparrow_j\downarrow_j - \Downarrow_j\uparrow_j\Big), \tag{17.147}$$

where the double and single arrows denote the localized moment and conduction electron, respectively, as illustrated in Figure 17.13(a).